ELSEVIER

Nuclear Instruments and Methods in Physics Research A 358 (1995) 323–326

NUCLEAR INSTRUMENTS & METHODS IN PHYSICS RESEARCH Section A

Resonator design and characterization for the Israeli tandem electrostatic FEL project ☆

I.M. Yakover, Y. Pinhasi, A. Gover *

Department of Physical Electronics, Tel-Aviv University, Ramat-Aviv, Israel

Abstract

The design and measurements of a resonator operating near 100 GHz and intended for use in a tandem FEL are presented. The designed resonator employs two parallel curved plates as a waveguide. In FEL operation the TE_{01} mode is excited. The resonator employs two wave splitters as reflectors. The wave splitters are segments of an overmoded rectangular waveguide which is connected at one end to the waveguide as described above, and is shorted at the other end by a metal plate with an aperture in the center for e-beam passage.

Gain calculations were made in the low gain regime. At the operating frequency the curvature of the plates and the gap size were chosen so as to maximize the gain.

A multimode analysis of the wave splitter was made. Calculations show, that the optimal splitter width and length allow achievement of very low diffraction losses at the aperture (~ 2%). This means that the aperture can be made sufficiently large to allow efficient beam entrance into the resonator without degrading its Q-factor.

A resonator prototype was constructed and its performance was evaluated experimentally.

1. Introduction

This paper deals with the theoretical and experimental investigations of the resonator designed for the Israeli tandem electrostatic FEL project. This FEL has the following basic parameters: e-beam energy $E = 1.5$–2.5 MeV, e-beam current $I_0 < 1$ A, wiggler magnetic field $B_w = 2$–3 kG, wiggler period $\lambda_w = 4.4$ cm, wiggler length $L_w = 88$ cm (20 periods), and the operating frequency is about 100 GHz.

At the beginning of this project several types of overmoded waveguides, i.e. rectangular, circular, and metal–dielectric waveguides [1] and waveguide formed by two parallel curved plates [2], were investigated theoretically in order to determine which of them allows one to reach the optimal performance. Numerical calculations were made taking into account two opposite requirements: that the dimensions of the waveguide cross-section be small enough so as to achieve large gain and be large enough for e-beam passage without interception. It was found that the mentioned set of parameters provides a maximal small signal gain of the order of 100% at the operating frequency of 100 GHz for all types of investigated waveguides.

The relatively low expected gain requires operation with a waveguide having low losses, which directed our choice to the parallel curved plates waveguide (see Fig. 1) in which the TE_{01} mode is excited. This waveguide has small ohmic losses and enables space for electron "wiggling" in the x-direction.

The reflector design also meets the difficulties resulting from the linear configuration of the tandem accelerator (see drawing presented in Ref. [3]). The reflectors must have a high reflectivity for the electromagnetic wave and be transparent to the e-beam. We have chosen a wave splitter proposed in Ref. [4] as a main reflector option. The wave splitter is a segment of the overmoded rectangular waveguide which is connected at one end to the parallel plate waveguide (see Fig. 1) and shorted at the other end by a metal plate with an aperture in the center for e-beam passage.

2. FEL gain consideration

Gain calculations were made using the following well known single-mode gain–dispersion equation [5] for the FEL operating in the linear regime:

$$G(s) \equiv \frac{(s - \mathrm{i}\theta)^2 + \theta_{\mathrm{pr}}^2}{s\left[(s - \mathrm{i}\theta)^2 + \theta_{\mathrm{pr}}^2\right] - \mathrm{i}Q}, \tag{1}$$

where

$$Q = I_0 \frac{e a_w^2 Z_s (k_z + k_w)^2 L_w^3}{8 m c A_{\mathrm{em}\,x}\, \omega_s \gamma^3 \gamma_z^2 \beta_z^3} \left[J_0(\rho) - J_1(\rho)\right]^2 \tag{2}$$

☆ This work was supported by grants of the U.S.–Israel Bi-National Foundation and the Israeli Ministry of Science.

* Corresponding author. Tel. +972 3 6 408 149, fax +972 3 6 423 508.

SSDI 0168-9002(94)01487-6

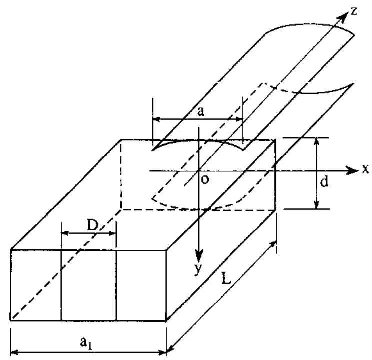

Fig. 1. Junction of wave splitter and parallel plate waveguide.

is the gain parameter,

$$\theta_{pr}^2 = \tilde{r}^2 \frac{eI_0}{\gamma_z^2 \gamma m \epsilon_0 V_z^3} L_w^2 \tag{3}$$

is the reduced space-charge parameter, $\tilde{r}$ is a plasma frequency reduction factor,

$$\theta = \left(\frac{\omega_s}{c} - k_z - k_w \right) L_w \tag{4}$$

is the detuning parameter, $a_w = eB_w/(k_w mc)$, $\gamma_z = \gamma/\sqrt{1 + a_w^2/2}$, $\beta = \sqrt{1 - 1/\gamma^2}$, $\gamma = 1 + E/(mc^2)$, $\beta_z = \sqrt{1 - 1/\gamma_z^2}$,

$$\rho = \frac{\omega_s}{8\beta k_w c} \left(\frac{a_w}{\beta\gamma} \right)^2 \left[1 - \frac{1}{2} \left(\frac{a_w}{\beta\gamma} \right)^2 \right]^{-3/2},$$

J_0, J_1 are Bessel functions, $k_w = 2\pi/\lambda_w$, and k_z, Z_s and $A_{em\,x}$ are the longitudinal wave number, wave impedance and effective mode area of the operating mode respectively. The effective mode area is determined by

$$A_{em\,x} = \frac{\int |E_x(x, y)|^2 \, dx \, dy}{|E_x(0, 0)|^2}, \tag{5}$$

where the integration is carried out over the waveguide cross-section and $E_x(0, 0)$ is calculated on the waveguide axis.

Electric field expressions were obtained in Ref. [2] analytically in the form of Gaussian–Hermite functions. For the case of a large curvature radius these expressions can be simplified, and the electric field profile of the TE_{01} mode has the form

$$E_x(x, y) = U_0 \cos\left(\frac{\pi y}{d} \right) e^{-x^2/w_0^2}, \tag{6}$$

where U_0 is the amplitude of the electric field, $w_0^2 = \sqrt{2Rd - d^2}/\kappa_{01}$,

$$\kappa_{01} = \frac{1}{d} \left[1 + \tan^{-1} \left(\frac{d}{\sqrt{2Rd - d^2}} \right) \right],$$

$Z_s = 120\pi/\sqrt{1 - (\kappa_{01} c/\omega)^2}$ is the wave impedance of the TE_{01} mode, and R is the curvature radius of the plates. Substituting expression (6) into (5) we obtain $A_{em\,x} = \sqrt{\pi}\, w_0 d/2^{3/2}$.

The calculated dependence of maximal gain (solid curves) and operating frequency (dotted curves) on e-beam energy are presented in Fig. 2. Calculations were made for the following parameters $R = 14.29$ mm, $B_w = 2$ kG, $L_w = 88$ cm, $\lambda_w = 4.4$ cm, $I_0 = 0.7$ A. As we may note, an operating frequency of 100 GHz can be obtained at low energies (1.3–1.6 MeV). The maximal gain decreases as the distance d between waveguide plates increases. Simulations of e-beam transport show that the spacing $d = 10$ mm is large enough for e-beam passage through the resonator without losses. This value of d allows achievement of maximal small signal gain of the order of 100% at the operating frequency of 100 GHz. Fig. 3 shows the gain frequency dependence calculated for this case.

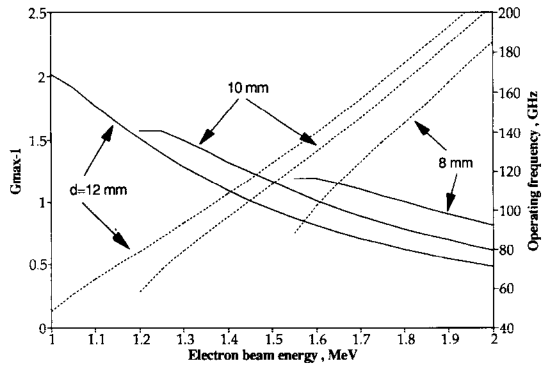

Fig. 2. The calculated dependence of maximal gain (solid curves) and operating frequency (dotted curves) on e-beam energy.

3. Wave splitter analysis

A multimode analysis of the wave splitter was carried out assuming that the tangential electric field in the plane

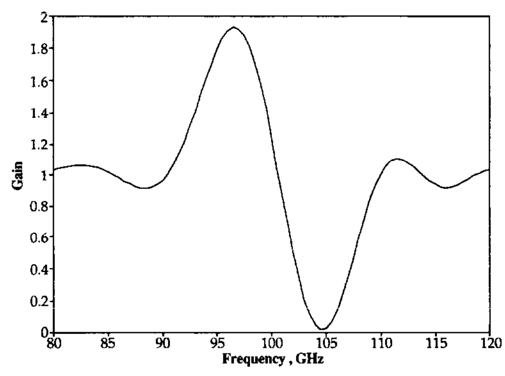

Fig. 3. Gain frequency response.

$z=0$ has the same profile as the electric field of the TE_{01} mode of the parallel curved plates waveguide. Further consideration was carried out for the case of a splitter of height equal to the distance between plates. This geometry allows one to assume that only the TE_{1n} and TM_{1n} modes are excited in the splitter waveguide. Their electric fields amplitudes are given by the expression (see Ref. [6])

$$U_{1n}^{p}=\int_{-a/2}^{a/2}\mathrm{d}x\int_{-d/2}^{d/2}\mathrm{d}y\,H_{y,1n}^{p}(x,\,y)E_x(x,\,y), \tag{7}$$

where $H_{y,1n}^{p}$ is the normalized magnetic field, p = h for the TE_{1n} modes, and p = e for the TM_{1n} modes.

Substitution of Eq. (6) into Eq. (7) results in

$$U_{1n}^{e}=U_0\frac{\alpha_n d}{2\chi_{1n}}\left(\frac{2\delta_n}{a_1 d}\right)^{1/2}(-1)^n V_n,$$

$$U_{1n}^{h}=U_0\frac{\pi}{\chi_{1n}}\left(\frac{2\delta_n}{a_1 d}\right)^{1/2}(-1)^n V_n. \tag{8}$$

Here

$$V_n=\int_{-a/2}^{a/2}\mathrm{d}x\,\cos(\alpha_n x)\,\mathrm{e}^{-x^2/w_0^2}, \tag{9}$$

and $\alpha_n=2n\pi/a_1$, $\chi_{1n}=(\alpha_n^2+(\pi/d)^2)^{1/2}$, $\delta_n=1$ for $n=0$ and $\delta_n=2$ for $n=1,2,\cdots$. Using Eq. (7) and (8) the power flow density can be represented in the form of a double series

$$P(x,\,y,\,z)=\tfrac{1}{2}\eta_0|U_0|^2\cos^2\left(\frac{\pi y}{d}\right)\times\frac{(\omega/c)^2-(\pi/d)^2}{a_1^2\omega/c}\tilde{P}(x,\,z),$$

$$\tilde{P}(x,\,z)=\mathrm{Re}\left\{\sum_{m=0}\sum_{n=0}\frac{\exp[\mathrm{i}(k_{1n}-k_{1m})z]}{k_{1n}}\delta_m\delta_n\times\cos(\alpha_m x)\cos(\alpha_n x)V_m V_n\right\}, \tag{10}$$

where $k_{1n}=((\omega/c)^2-\chi_{1n}^2)^{1/2}$, $\eta_0=1/120\pi$, and only propagating modes are considered.

The results of the computation of $\tilde{P}(x,\,z)/\tilde{P}(0,\,0)$ for $d=10$ mm, $a=22$ mm, $R=14.29$ mm, $f=100$ GHz, and $a_1=25$ mm are shown in Fig. 4 for various lengths of the wave splitter. As we see, at the optimal distance z the electromagnetic field is negligibly small in a large part of the splitter cross-section. Similar results were achieved in Ref. [4]. This means that the electromagnetic wave and the electron beam can be successfully separated in this plane by shorting the wave splitter by a metal plate having an aperture in its center.

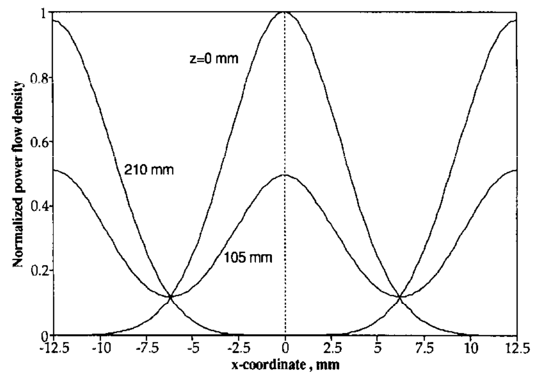

Fig. 4. Calculations of normalized power flow density in a wave splitter.

Diffraction losses in the aperture can be estimated by calculating the ratio

$$\frac{W_a}{W}=\frac{\int_{S_a}P(x,\,y,\,z)\,\mathrm{d}x\,\mathrm{d}y}{\int_{-a_1/2}^{a_1/2}\mathrm{d}x\int_{-d/2}^{d/2}\mathrm{d}y\,P(x,\,y,\,z)}, \tag{11}$$

where W_a is the power flow through the aperture of area S_a, and W is the incident power flow. For the aperture in the form of a rectangular slot of the width D and of the length d (see Fig. 1) this ratio can be found analytically:

$$\frac{W_a}{W}=\mathrm{Re}\left\{\sum_{m=0}\sum_{n=0}\delta_m\delta_n V_m V_n\frac{\exp[\mathrm{i}(k_{1n}-k_{1m})z]}{k_{1n}}\times[\varphi(\alpha_{n-m})-\varphi(\alpha_{n+m})]\Big/\left[a_1\sum_{n=0}\frac{\delta_n V_n^2}{k_{1n}}\right]\right\}, \tag{12}$$

where $\varphi(\alpha_n)=(\sin(\alpha_n D/2))/\alpha_n$.

Fig. 5 shows the dependence of W_a/W on frequency, calculated for the parameters $d=10$ mm, $a_1=25$ mm, $L=210$ mm and various values of the aperture size parameter D. As we see a slot having a width $D=10$ mm

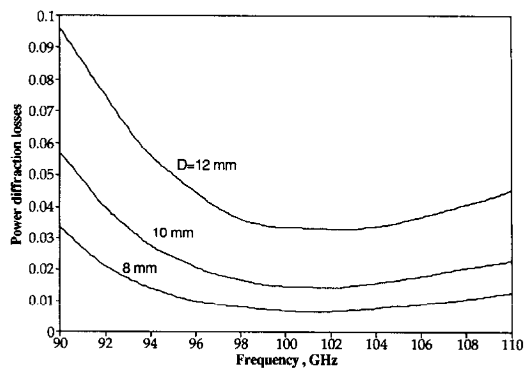

Fig. 5. Calculated diffraction losses in an aperture.

provides very low diffraction losses (of the order of 2% in the frequency band 96–106 GHz).

4. Experimental results

The resonator prototype was designed and built on the basis of theoretical investigations described above. The waveguide samples have a curvature radius of $R = 14.75$ mm and a spacing between plates of $d = 10.7$ mm. This value of d was chosen in order to use the standard tapered transition between W-band and K-band waveguides. The input cross-section of this transition has the dimensions 2.54×1.27 mm^2 and the output cross-section is 10.7×4.3 mm^2. It provides for good mode matching in the y-direction and therefore the TE_{01} mode of a parallel plate waveguide can be excited efficiently.

In order to determine the waveguide attenuation constant, the transmission coefficient was measured. Two samples of the same length 400 mm and of different widths of their curved parts $a = 15$ mm and $a = 22$ mm were tested. The results of transmission coefficient measurements made for the waveguide with $a = 15$ mm are shown in Fig. 6. The observed deep oscillations are the result of mismatching between the tapered transition and the tested waveguide in the x-direction and multiple reflections of the electromagnetic wave. Positions of maxima and minima were measured directly using a frequency meter. Numerical analysis allows one to determine the transverse wave number κ of the observed mode; it was found that $\kappa = 0.35$ 1/mm while the calculated value is $\kappa_{01} = 0.36$ 1/mm. Good agreement between theoretical and experimental values leads to the conclusion that the observed mode is the TE_{01} mode.

Further numerical analysis of the experimental results was made in the single mode approximation, and the attenuation constant was determined. The asterisks in Fig. 7 present the attenuation constant of a waveguide having a = 15mm. As we see the attenuation constant is relatively large of the order of 3 dB/m. This can be understood if one notes that the waveguide width is smaller than the

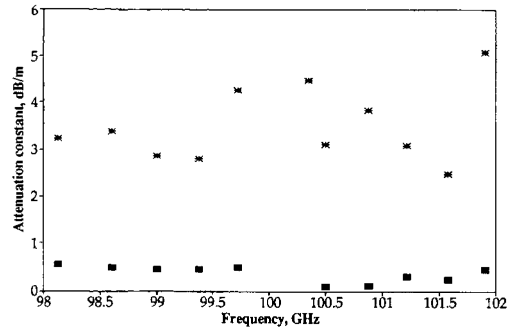

Fig. 7. Waveguide attenuation constant.

TE_{01} mode spot size on the curved plate which leads to significant diffraction losses.

Diffraction losses can be reduced by utilizing the wider waveguide. The waveguide sample having $a = 22$ mm was tested, and its attenuation constant is depicted in Fig. 7 by the squares. This waveguide sample has much smaller losses than the first one, and the lowest attenuation constant of the order of 0.1 dB/m as observed at frequencies of 100.5 and of 100.8 GHz.

A wave splitter having cross-section dimensions of 10.7×25 mm^2 and a length of $L = 210$ mm was built and tested experimentally. First the influence of the aperture in the shorting plate was examined. For this purpose the results of the wave slitter reflection coefficient measurements made for the splitter shorted by a metal plate with a circular aperture of 10 mm diameter were compared with the results obtained for the splitter shorted by a full plate without any aperture. A full coincidence of the results was observed, indicating that the reflectivity of the apertured short is as high as the full short within the measurement accuracy. The return loss of the splitter was also measured. As a reference the return loss of the shorted parallel plate waveguide was used. Very low return loss (< 0.1 dB) was observed at frequencies of 99.8, 100.3, 100.9, 101.3 and 102 GHz. This means that the round trip power loss is of the order of 0.35 dB (8%) for our resonator with a waveguide of 88 cm length. This loss value corresponds to a Q-factor of the order of 20000, a very high value for a 100 GHz resonator.

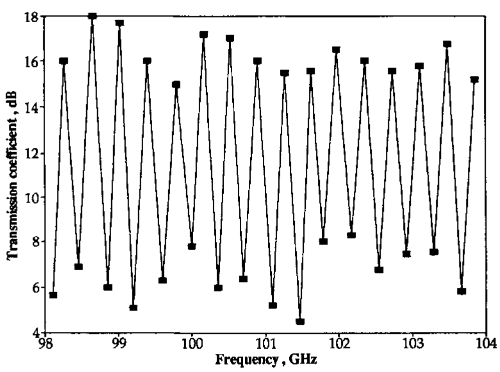

Fig. 6. Measurements of waveguide transmission.

References

[1] Yu.N. Kazantsev, Sov. Radio Eng. Elec. Phys. 15 (1970) 963.
[2] T. Nakahara and N. Kurauchi, IEEE Trans. MTT-15 (1967) 66.
[3] A. Gover et al., Nucl. Instr. and Meth. A 341 (1994) ABS 57.
[4] W.H. Urbanus et al., Nucl. Instr. and Meth. A 331 (1993) 235.
[5] Y. Pinhasi et al., Nucl. Instr. and Meth. A 318 (1992) 523.
[6] Kh.L. Garb, P.Sh. Fridberg and I.M. Yakover, Sov. Phys. Collection 22 (1982) 27.